Interacting multiple model-based human motion prediction for motion planning of companion robots*

Donghan Lee[1], Chang Liu[2] and J. Karl Hedrick[3]

Abstract— **Motion planning of human-companion robots is a challenging problem and its solution has numerous applications. This paper proposes a motion planning method for human-companion robots to accompany humans in a socially desirable manner, which takes into account the safety, comfortableness and naturalness requirements. A unified Interacting Multiple Model (IMM) framework is developed to estimate human motion states from noisy sensor data and predict human positions in a finite horizon. The robot motion planning is formulated as a model predictive control problem to generate socially desirable motion behavior based on the predicted human positions. The effectiveness of the proposed motion planning method in facilitating the socially desirable companion behavior is evaluated through simulations and the advantage of IMM framework for human motion estimation and prediction compared to traditional single-model approaches has been demonstrated.**

I. INTRODUCTION

The application of autonomous robots for search-and-rescue (SAR) missions have received considerable attentions in last decades [**?**], [**?**], [**?**]. One particular interesting scenario is allowing autonomous robots to accompany humans during the SAR. Robot companions can follow and assist humans in carrying heavy apparatus, exploring dangerous areas or detecting signals of survivors.

Socially desirable companion behavior necessitates several requirements to be satisfied, including safety, comfort, naturalness and sociability [1]. Among these requirements, safety serves as the fundamental guideline, requiring that robots avoid collision with accompanied humans under all circumstances [2]–[4]. Comfort composes a social requirement on the robot behavior, which requires robots to pose little annoyance and stress for the accompanied humans [1]. It is mainly formulated regarding the distance that a robot needs to keep from people. For example, Hall [5] proposed the concept of "Proxemics" to denote the virtual zone around a person that other people should avoiding entering in order to prevent the discomfort the person may feel. Barnaud et al. [6] investigated the proxemics models in the context of human-aware robot navigation by investigating a classic corridor-crossing experiment. This work provides a tool for designing parameters of the proxmics model that can be used for robot motion planning in the environment with human existence.

To generate socially desirable motion behavior, accurate human motion estimation and prediction is necessary, which can be then utilized for robot motion planning. To be specific, a robot needs to estimate motion states of the accompanied human in real time based on measurements from equipments such as GPS sensors or cameras and then predict human future trajectory. Traditional filtering methods, such as the Kalman filter (KF), has been applied for tracking moving objects Huang et al. [**?**], [7], [8]. Simple human motion models, such as the constant speed and direction model, has been utilized in [4], [9]. These approaches can efficiently track humans when the people follow the assumed motion pattern. However, when humans movement involves complex behaviors (such as making turns), such methods may fail.

Learning techniques have also been utilized for human motion prediction in recent years. Bennewitz et al. [10] proposed a technique for learning collections of trajectories that characterize typical motion patterns of persons Trajectories were clustered using the Expectation Maximization algorithm and a hidden Markov model was then applied to predict future positions of persons. Fulgenzi et al. [11] developed an approach for predicting trajectories of moving objects, using typical motion patterns that were pre-learned based on the collected set of trajectories and represented by Gaussian processes. A two-layer prediction that combined long-term destination inference and short-term motion prediction was proposed in [12]: the short-term prediction was achieved by a Polynomial Neural Network (PNN), which was trained offline; the long-term prediction was performed by utilizing the heading direction of a human to determine the destinations where he/she would have interest in visiting.

These approaches have achieved success in predicting human motion trajectories. However, they usually involves the collection of training data (e.g., recorded human trajectory) and are prone to be scenario specific. In fact, human motion can be well predicted using these learning-based approaches in the environments where human trajectories have been collected for training predictors. However, these predictors may fail to obtain accurate prediction in unknown environments. This drawback renders the learning-based methods less applicable for SAR missions since disaster sites are diverse and rarely similar to the known ones. Therefore robots need to work in unfamiliar environments.

In this work, we propose an Interacting Multiple Model (IMM)-based human motion prediction approach, taking

*This work was not supported by any organization

[1]Donghan Lee with the Vehicle Dynamics & Control Lab, Department of Mechanical Engineering, University of California at Berkeley, California 94720, USA donghan.lee@berkeley.edu

[2]Chang Liu with the Vehicle Dynamics & Control Lab, Department of Mechanical Engineering, University of California at Berkeley, California 94720, USA changliu@berkeley.edu

[3]J. Karl Hedrick is with Faculty of Mechanical Engineering, University of California at Berkeley, California 94720, USA khedrick@berkeley.edu

advantage of the fact that human motion usually involves different identified motion models [13], such as straight-line movement, making turns and change of speed. Such IMM-based predictor incorporates several motion models into account and dynamically adjusts the mode probabilities based on the observed human trajectory. To deal with the nonlinearity of the human motion (such as making turns), Unscented Kalman Filter is applied to each model in the IMM framework, resulting in the so-called IMM-UKF approach. Such approach can achieve higher prediction accuracy compared to traditional methods that utilizes a single motion model. Additionally, no training is needed and thus scenario-independent, which is advantageous over learning-based methods for search and rescue missions.

Based on the predicted human trajectory, robot motion planner that generates socially desirable companion behavior is necessary. Several motion planner have been proposed in previous work. For example, Hoeller et al. [2] presents a local path planning approach based on the expansive-spaces tree algorithm, which repeatedly computes collision-free paths from the robots current position to a target position near the person using a randomized search in configuration space. Fulgenzi et al. [11] proposed an extended Rapidly-exploring Random Tree (RRT) algorithm that takes the likelihood of the obstacles trajectory and the probability of collision into account for robot path planning in a dynamic uncertain environment. Similar RRT approaches have also been adopted in [6], [14].

In this work, a model predictive control (MPC)-based motion planner is developed that formulates the motion planning as a nonlinear programming that considers the safety and comfort requirements. Such approach offers the flexibility in incorporating diverse constraints on motion dynamics and motion behavior and can be solved online.

The main contribution of this paper is ... (**TODO:** need to fill this paragraph).

The remainder of this paper is organized as follows: first, the problem of motion planning for a human-companion robot is formulated for the SAR mission; second, the IMM-UKF estimation and prediction method is described, followed by the MPC planner; next, simulation setup and results on evaluating the proposed approach are presented; lastly, concluding remarks and ideas of future work are presented.

II. PROBLEM FORMULATION

Consider the SAR scenario (Fig. 1) in which a human first responder needs to deliver medical treatment to several destinations that contain injured people. A companion robot that carries medical apparatus will accompany the human and sequentially move to these destinations. The robot has no knowledge about the positions of human destinations. However, it can measure human positions in real time from the GPS sensor that the human carries.

The robot motion capability is modeled by the following

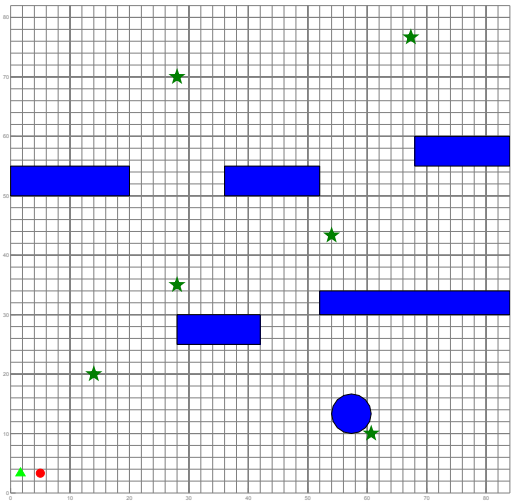

Fig. 1: A search-and-rescue scenario for the companion robot to accompany a human. The red circle and the green triangle represent the human rescuer and the robot companion, respectively. Stars denote human destinations and the blue rectangles stand for static obstacles.

kinematic model:

$$p^r(k+1) = p^r(k) + v^r(k) \begin{bmatrix} \cos\theta(k) \\ \sin\theta(k) \end{bmatrix} T \tag{1a}$$

$$v^r(k+1) = v^r(k) + a(k)T \tag{1b}$$

$$\theta^r(k+1) = \theta^r(k) + w(k)T \tag{1c}$$

$$a_{lb} \leq a^r(k) \leq a_{ub} \tag{1d}$$

$$w_{lb} \leq \omega^r(k) \leq w_{ub} \tag{1e}$$

where $(p^r(k), v^r(k), \theta^r(k))$ denote the robot state at time k, representing the position, speed and heading angle, respectively; T represent the discretization sampling time. The control input consists of the acceleration $a^r(k)$ and the angular velocity $\omega^r(k)$, with a_{lb}, w_{lb} being the corresponding lower bounds and a_{ub}, w_{ub} the upper bounds.

Several obstacles exist in the field, including five stationary ones and two moving ones, representing unmovable obstructions, such as buildings or plants, and mobile objects, such as pedestrians or vehicles, respectively. The positions of stationary obstacles are known to both the human and the companion robot while the moving obstacles are measured using same measurement tool for tracking the human rescuer(**TODO:** How to make is reasonable that moving obstacles also have GPS?). When accompanying the human, the robot should satisfy the aforementioned safety and comfort requirements. To be specific, a circular "safety zone" with radius d_s (**??**) is defined around the target person. Stepping into the"safety zone" is considered as unsafe behavior and thus should be avoided. The comfort requirement consists of two parts: the robot needs to maintain a comfortable distance d_c from the human, as investigated in [5], and also keep similar speed with the human, as shown in [**?**].

III. METHODS

A. Human Motion Estimation

The Interacting Multiple Model (IMM) approach are applied for estimating the human motion from the noisy sensor data. It utilizes a bank of r number of filters corresponding to different motion models. State estimate at time k is computed as a weighted sum of estimates from each filter, as shown in the following formula:

$$\hat{x}(k|k) = \sum_{j=1}^{r} \mu_j(k)\hat{x}^j(k|k)$$

where r denotes the number of models; $\hat{x}^j(k|k)$ represents the state estimate from the j^{th} filter; $\mu_j(k)$ stands for the mode probability and is computed as follows:

$$\mu_j(k) = \frac{1}{c}\sum_{i=1}^{r} L_{ij}(k)p_{ij}\mu_j(k-1)$$

where c denotes the normalizing factor; $L_{ij}(k)$ stands for the likelihood function and p_{ij} represents the mode transition probability from the i^{th} to the j^{th} model. Each filter uses the mixed initial state estimate and covariance from different combination of the previous model. Readers interested in the details of the IMM approach can refer to [**?**].

In this work, two different dynamic models are used in the IMM framework: one is the coordinated turn motion model, reflecting the action of making turns or moving along a curved path, and the other is the uniform motion model, representing the straight-line movement. The equation of motion for the coordinated turn motion becomes the following

$$x^{h,1}(k+1) = f(x^{h,1}(k)) + Gw(k) \tag{2a}$$

$$f(x^{h,1}(k)) = \begin{bmatrix} p_1^h + \frac{\sin(\omega^h T)}{\omega^h}v_1^h - \frac{1-\cos(\omega^h T)}{\omega^h}v_2^h \\ \cos(\omega^h T)v_1^h - \sin(\omega^h T)v_2^h \\ p_2^h + \frac{1-\cos(\omega^h T)}{\omega^h}v_1^h + \frac{\sin(\omega^h T)}{\omega^h}v_2^h \\ \sin(\omega^h T)v_1^h + \cos(\omega^h T)v_2^h \\ \omega^h \end{bmatrix} \tag{2b}$$

$$G = \begin{bmatrix} \frac{T^2}{2} & 0 & 0 \\ T & 0 & 0 \\ 0 & \frac{T^2}{2} & 0 \\ 0 & T & 0 \\ 0 & 0 & 1 \end{bmatrix} \tag{2c}$$

$$w \sim \mathcal{N}(0, Q) \tag{2d}$$

Also, the equation of the uniform motion is represent as follows:

$$\dot{x}^{h,2}(k+1) = Ax^{h,2}(k) + Bw(k) \tag{3a}$$

$$A = \begin{bmatrix} 1 & T & 0 & 0 & 0 \\ 0 & 1 & 0 & 0 & 0 \\ 0 & 0 & 1 & T & 0 \\ 0 & 0 & 0 & 1 & 0 \\ 0 & 0 & 0 & 0 & 0 \end{bmatrix}, \; B = \begin{bmatrix} \frac{T^2}{2} & 0 & 0 \\ T & 0 & 0 \\ 0 & \frac{T^2}{2} & 0 \\ 0 & T & 0 \\ 0 & 0 & 1 \end{bmatrix} \tag{3b}$$

where $x^{h,i}(k)$ represents the human motion state including five elements : $p_1^h, v_1^h, p_2^h, v_2^h, \omega^h$, where p_1^h, p_2^h denote the longitudinal and lateral position of the human, v_1^h, v_2^h the corresponding velocity and ω^h the turn rate of the human; $w(k)$ represents process noise; T represents the sampling time; Q is the covariance matrix of the process noise.

The uniform motion model is essentially a special case of the coordinated turn motion model with the turn rate ω being fixed to zero. It seems that only considering the coordinated turn motion model suffices to estimate human motion states, in addition to the benefits of reduced computations by using the single model. However, including two models are necessary since this allows the estimator for fast detection of change of motions. The decision to select the estimator is a bit clearer in linear case since the turn rate is fixed in linear dynamic models. In other words, the diverse turn rate allows that the estimation of the human motion is more accurate.

With a single nonlinear model, it is possible to provide accurate state estimates. However, it is common to include one uniform motion model and one coordinated turn motion model for quick motion-change detection. Since human motion usually involves different motions in the real world, the ability to quickly detect the change of the motion is one of the important properties for the estimation and prediction.

The observation equation is represented as :

$$y^h(k) = Cx^h(k) + v(k) \tag{4a}$$

where $y^h(k)$ denotes the observed human state at the time step k; $v(k)$ stands for measurement noise.

By using GPS sensors or cameras, the human positions can be measured. Therefore, the parameters in observation model Eq. (4a) is defined as:

$$C = \begin{bmatrix} 1 & 0 & 0 & 0 & 0 \\ 0 & 0 & 1 & 0 & 0 \end{bmatrix}, \tag{5a}$$

$$v \sim \mathcal{N}(0, V) \tag{5b}$$

where V is the convariance matrix of the measurement noise. The above two models are utilized for human motion state estimation, in combination with the Unscented Kalman Filter.

B. Unscented Kalman Filter

The Unscented Kalman Filter (UKF) is applied to each model that are used in IMM framework for estimating human states. It is an effective state estimation technique for nonlinear systems by implementing the Unscented Transformation (UT) that calculates the statistics of a random vector that undergoes a nonlinear transformation [**?**]. To be specific, given an arbitrary nonlinear dynamic model $z = f(x)$ and as L-dimensional Gaussian Random Vector (GRV) x with mean $\hat{x}$ and covariance P_x(**TODO:** how to choose the mean and Covariance), the statistics of z can be approximated by using $2L+1$ discrete sample points $\{\chi^{(i)}\}_{i=0}^{2L} = \{\hat{x} \text{ and } \hat{x} \pm \sigma_j, j = 1, ..., L\}$, called *sigma points*, where σ_i is the i^{th} column of the matrix $\sqrt{(L+\lambda)P_x}$. λ is a scaling

parameter, as defined below:

$$\lambda = \alpha^2(L+\kappa) - L \tag{6a}$$
$$W_0^{(m)} = \frac{\lambda}{L+\lambda} \tag{6b}$$
$$W_0^{(c)} = \frac{\lambda}{L+\lambda} + 1 - \alpha^2 + \beta \tag{6c}$$
$$W_i^{(m)} = W_i^{(c)} = \frac{1}{L+\lambda}, \quad i = 1, ..., 2L \tag{6d}$$

where α determines the spread of sigma points about the mean $\hat{x}$; κ is a secondary scaling parameter; β is used to incorporate prior knowledge of the distribution.

Once the sigma points have been generated, each point is passed through the nonlinear function $z = f(x)$, i.e. each column of the sigma points is propagated through the nonlinearity, as in $\zeta = f(\chi), i = 0, ..., 2L$. The mean $\hat{z}$ and the covariance P_z are approximated as $\hat{z} \simeq \Sigma_{i=0}^{2L} W_i^{(m)} \zeta^{(i)}$ and $P_z \simeq \Sigma_{i=0}^{2L} W_i^{(c)} (\zeta^{(i)} - \hat{z})(\zeta^{(i)} - \hat{z})^\mathsf{T}$, calculated as given in above equations of the weights and parameters [**?**]. Readers can refer to [**?**] for more details of the UKF algorithm.

C. Human Motion Prediction

The estimated human motion states and the mode probabilities are utilized for predicting human future states. To be specific, using the uniform motion model and the turn motion model, human positions for each model can be extrapolated and then combined based on the mode probabilities to obtain the predicted positions. Let $\hat{x}^{h,j}(k|k)$ and $\tilde{x}^{h,j}(k+i|k)$ represent the estimated and predicted human states associated with the j^{th} model at time k and $k+i\,(i \geq 0)$, respectively, based on the observations up to time k. The prediction procedure works as follows:

[Note:] what's the difference between two sides of Eqn. (6c)?

$$\tilde{x}^h(k+l+1|k) = \sum_{j=1}^{r} \mu_j \tilde{x}^{h,j}(k+l+1|k) \tag{7a}$$
$$l = 0, \ldots, N-1 \tag{7b}$$
$$\tilde{x}^{h,j}(k+l+1|k) = \hat{x}^{h,j}(k+l+1|k) \quad j = 1, \ldots, r \tag{7c}$$
$$= \Sigma_{i=0}^{2L} W_i^{(m)} \chi_{k+l+1|k}^{(i)} \tag{7d}$$
$$\chi_{k+l+1|k}^{(i)} = f(\chi_{k+l|k}^{(i)}) \quad i = 0, \ldots, 2L \tag{7e}$$

where N denotes the prediction horizon; r represents the number of models; L is the dimension of $x^{h,j}$. For the purpose of simplicity, we define $p^h(k) = \begin{bmatrix} p_1^h(k) \\ p_2^h(k) \end{bmatrix}$ and $v^h(k) = \left\| \begin{bmatrix} v_1^h(k) \\ v_2^h(k) \end{bmatrix} \right\|_2$ to represent the position vector and the speed of the human at time k, respectively. Notations for the estimated and predicted position vector and speed can be defined as $\hat{p}^h(k|k), \tilde{p}^h(k+i|k), \hat{v}^h(k|k), \tilde{v}^h(k+i|k)$, respectively.

D. Robot Path Planning

The model predictive control (MPC) approach i utilized for robot motion planning. MPC provides an effective framework for incorporating the safety and comfort requirements into the planning procedure. It iteratively solves a finite-horizon constrained optimal control problem. After obtaining the optimal control inputs over the planning horizon, it implements the first input and then computes for a new set of control inputs, starting from the updated state. The optimal control inputs are obtained by solving a nonlinear programming problem that incorporates the kinematics of the robot and the safety and comfort requirements:

$$\min_{\mathbf{A}_k, \mathbf{\Theta}_k} \quad \sum_{i=1}^{N} q_1 \left| \left\| \bar{p}^r(k+i|k) - \tilde{p}^h(k+i|k) \right\|_2^2 - d_c^2 \right| + q_2 \left| \bar{v}^r(k+i|k) - \tilde{v}^h(k+i|k) \right|^2 \tag{8a}$$

subject to Robot kinematic model: Eqs. (1a) to (1e)

$$||\bar{p}^r(k+i+1|k) - \tilde{p}^h(k+i+1|k)||_2 \geq d_s \tag{8b}$$
$$||\bar{p}^r(k+i+1|k) - \tilde{p}_{l_m}^{obs_m}(k+i+1|k)||_2 \geq d_s \tag{8c}$$
$$h_{l_s}(\bar{p}^r(k+i+1|k)) \geq 0 \tag{8d}$$
$$h_{l_s}(\lambda \bar{p}^r(k+i|k) + (1-\lambda)\bar{p}^r(k+i+1|k)) \geq 0 \tag{8e}$$
$$\forall l = 1, \ldots, m,\ 0 \leq \lambda \leq 1$$
$$\bar{p}^r(k|k) = p^r(k) \tag{8f}$$
$$\bar{v}^r(k|k) = v^r(k) \tag{8g}$$
$$\bar{\theta}^r(k|k) = \theta^r(k) \tag{8h}$$

where $\bar{p}^r(k+i|k)$, $\bar{v}^r(k+i|k)$ and $\bar{\theta}(k+i|k)$, $0 \leq i \leq N$ represent the planned position, speed and heading angle at time $k+i$, respectively; N is the prediction horizon. n_s is the number of static obstacles and $p_{l_s}^{obs_s}$ denotes the position of the l_s^{th} obstacle; n_m stands for the number of moving obstacles and $p_{l_m}^{obs_m}$ and $r_{l_m}^{obs_m}$ denote the position and the radius of the l_m^{th} obstacle; $(\mathbf{A}_k, \mathbf{\Theta}_k)$ stand for the set of optimal acceleration and angular velocity in the prediction horizon $[k, k+N-1]$, obtained by solving the above optimization problem at time k.

The objective function Eq. (8a) consists of two terms: the first one stands for the difference between the squared human-robot distances and the squared comfort distance; the second one represents the speed difference between the robot and the human. This reflects the comfort requirement that the robot maintain the comfort distance from the human and keep similar pace at the same time. q_1 and q_2 denote the weights for these two terms. The safety constraints are imposed in Eqs. (8b) to (8e). Eqs. (8b) and (8c) regulates that the robot stay at least the safety distance d_s from the human and moving obstacles in order to avoid collision. To avoid moving obstacles, the same motion prediction method described in Section III-C is applied **????** enforce the collision avoidance with static obstacles. To be specific, Rectangular obstacles are approximated by ellipsis, the details of

which are described in the Appendix. Let h_{l_s} represent the analytical epxeression of the ellipse approximation of the l_s^{th} obstacle. **??** demands that each way point of the robot be kept outside of static obstacles. And **??** requires that the trajectory connecting the adjacent way points not intersect with obstacles, which eliminates the waypoints that leads the robot across obstacles. Eqs. (8f) to (8h) initializes the robots planned states based on its actual state at time k.

IV. SIMULATION RESULTS & DISCUSSION

A. Simulation setup

Simulations have been run to evaluate the proposed robot motion planning approach. A human rescuer will move sequentially to five targets in a $84m \times 82m$ field, following the trajectory as shown in Fig. 6c. Notice that such trajectory covers several typical human motion patterns, including straight-line movement, motion following curved paths and making sharp turns. Therefore, it provides a realistic benchmark for evaluating the proposed motion planning approach. The trajectory is unrevealed to the robot. The human speed is set to be constant at $1.5m/s$. The safety distance d_s is chosen as $1m$. According to the research by Hall et al., the comfort distance between two acquaintances ranges from 1.2m to 3.6m [5]. In the simulation, we choose d_c as $2.4m$. However, any distance within this range is considered a comfortable one. The sampling rate of GPS sensor is $20Hz$ and the variance of sensor measurement noise is considered as $2m$. The robot's maximum acceleration and deceleration are set to be $1m/s^2$ and $-3m/s^2$ respectively and the angular velocity range is chosen to be $[-90°/s, 90°/s]$. In the IMM estimator, the process noise and the measurement noise are set to be 1.5×10^{-2} and 1.5, respectively. The parameters of UKF in the estimator are $L = 5, \alpha = 0.001, \kappa = 0$ and $\beta = 2$. The prediction horizon for the human motion is chosen as $500ms$ and the robot iteratively computes the control inputs every $500ms$.

B. Simulation results

Figs. 6a and 6b show both the human and robot's trajectories by the time the screenshots are made.

The performance of human motion estimation and prediction is evaluated by comparing with three other predictors. The MPC-based robot motion planning method is then evaluated using different prediction strategies.

1) Human motion estimation: The error between the estimated and the actual human position and speed at each time step are compared to evaluate the estimation accuracy. The position error vector can be formulated as:

$$\Delta_p^t(k) = p^h(k) - \hat{p}^h(k|k)$$

where $p^h(k)$ denotes the actual human position at time k.

Fig. 2 shows the position estimation error on longitudinal and lateral directions using four different estimators: Linear Kalman Filter (LKF), IMM-LKF, UKF and IMM-UKF. In the simulation, the same turn motion model in IMM-UKF is adopted for the system dynamics in UKF; the uniform motion model in IMM-LKF is also applied to the

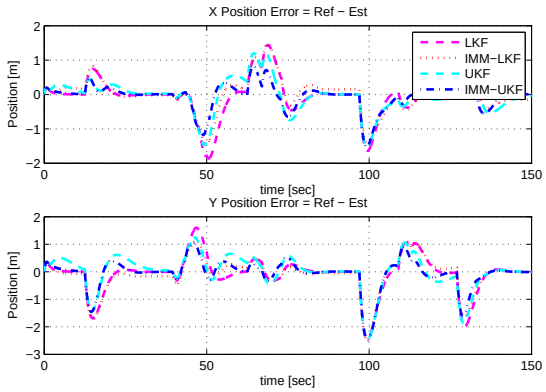

Fig. 2: Comparison of position estimation error with LKF, IMM-LKF, UKF and IMM-UKF

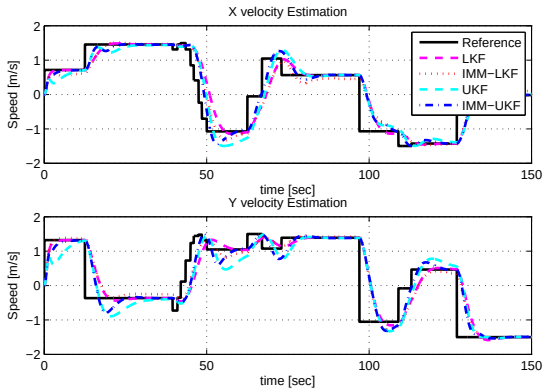

Fig. 3: Comparison of the estimated velocity using the IMM-based and the single-model approaches

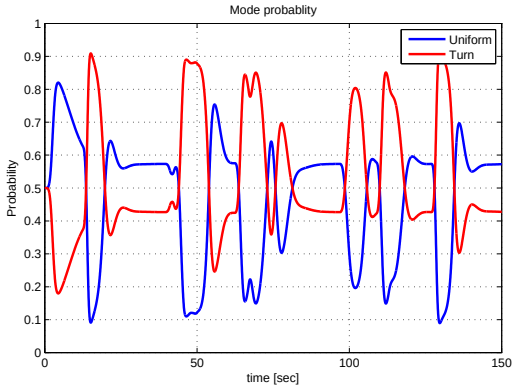

Fig. 4: Model probabilities of two models in the IMM-UKF estimator

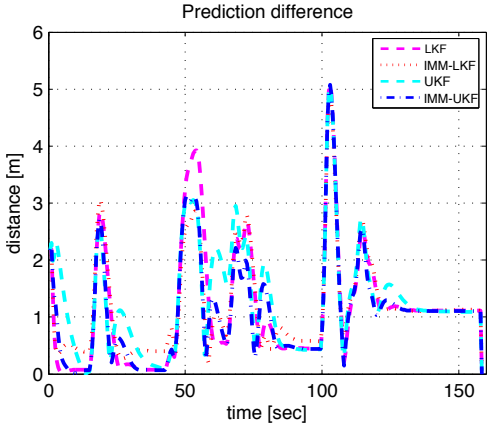

Fig. 5: Comparison of prediction error between the IMM-based and single-model approaches

dynamic model in LKF. Two observations can be obtained in this figure. First, the responses of the nonlinear estimators such as UKF and IMM-UKF are faster than the linear estimators. Second, the IMM-based approaches show better performance in accuracy than the single-model approaches. Besides, IMM-UKF achieves the fastest response and best accuracy compared to other methods, especially when the human turns around the circular obstacle at time 50. Fig. 3 compares the velocity estimation using four estimators. Overall, the nonlinear estimators (UKF and IMM-UKF) show faster response compared to the linear estimators (LKF and IMM-LKF), though they have overshoots due to the fast response. It is worth noting that the overshoots of IMM-UKF are smaller than UKF while keeping the fast response at time 53 and 118 when the velocity changes abruptly. This makes sense as the UKF-IMM estimator incorporates uniform motion model that can capture the sudden velocity changes. Fig. 4 shows the mode probabilities of the uniform motion model and turn motion model in IMM-UKF over time. When the human speed changes, the mode probability of the turn motion becomes higher than that of the uniform motion. These changes illustrates the reason that IMM-based estimators achieve more accurate and faster estimation than the single-model estimator at the sharp turn and circular turn, thus demonstrating the necessity of applying IMM-UKF estimator for human tracking.

2) Human motion prediction: To evaluate the IMM-based prediction approaches(IMM-LKF and IMM-UKF), the average prediction error over the prediction horizon is computed and compared with the single-model approaches (LKF and UKF). At time k, the prediction error is defined as:

$$\Delta_p(k) = \frac{1}{N}\sum_{i=1}^{N} ||\tilde{p}^h(k+i|k) - p^h(k+i)||_2 \qquad (9)$$

Different from the IMM-based prediction approaches that extrapolate the human position by a weighted sum of the predicted positions from each model, the single-model methods only utilize the uniform motion model for prediction.

Fig. 5 shows the comparison of prediction error using two single-model approaches (LKF, UKF) and two IMM-based methods (IMM-LKF, IMM-UKF). It can be noticed that single-model approaches generate larger prediction error than IMM-based methods, especially when the human makes turns, such as at time 50. This makes sense as IMM-based methods have already considered such turn motion model. Based on the simulation results, IMM-UKF is shown to outperform the other three prediction approaches.

TABLE I: Human-robot Distance

Method	IMM-UKF	UKF	non-prediction
Ave	2.716	2.8774	3.8913
Std	0.9084	0.8548	0.6549

TABLE II: Speed Difference

Method	IMM-UKF	UKF	non-prediction
Ave	0.0789	0.1057	0.0008
Std	0.2559	0.2583	0.1868

3) Robot motion planning: Fig. 6d shows the trajectory of the companion robot that accompanies the target person moving in the field. The trajectory is generated by the proposed MPC motion planner with five-step planning horizon ($2.5s$) and using the IMM-UKF for predicting the human and moving obstacles' trajectories. The performance of the motion planning is evaluated using the criterion of safety (**TODO:** need to evaluate the safety in the following paragraphs) and comfort. To be specific, the distance and speed differences between the robot and the human at each time step are measured, which are defined as:

$$\Delta_d(k) = ||p^r(k) - p^h(k)||_2 \qquad (10a)$$

$$\Delta_v(k) = |v^r(k) - v^h(k)| \qquad (10b)$$

These quantities are illustrated as the blue line in Figs. 7 and 8.

The performance of IMM-UKF predictor for robot motion planning compared with two benchmark prediction strategies, using the same MPC planner. The first benchmark method uses the coordinate turn motion model and applies a single-model predictor (the UKF predictor) to

[Note:] Dong-han, is this correct?

predict human motion. The second method does not predict human motion. Instead, the robot only utilize the human's current state for one-step ($500ms$) motion planning.

Fig. 7 compares the distances between the human and the robot using these three strategies. It can be noticed that the MPC planner has ensured the safety of the accompanied human with each of the three prediction methods in that no distance goes below d_s. Additionally, by incorporating human motion prediction into the motion planning, the robot significantly improves its companion performance from the non-prediction case. This can be demonstrated by Table I that the mean of human-robot distance using the prediction is much smaller than that without prediction. Additionally, the IMM-UKF predictor achieves better performance than the UKF-predictor in that the average distance is smaller

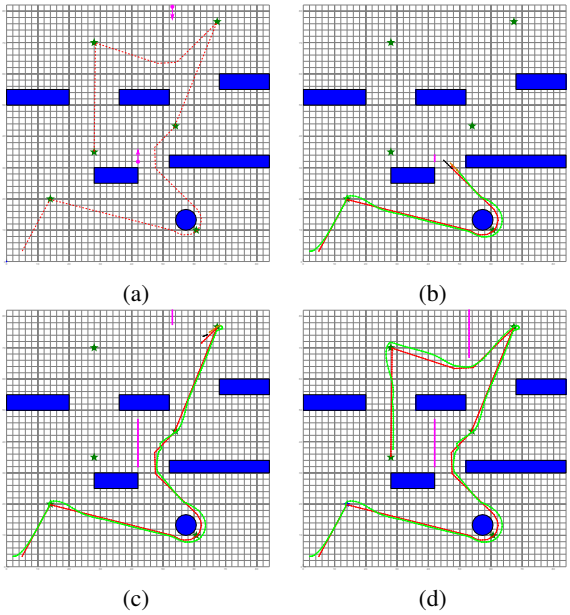

Fig. 6: A screenshot of the simulation. The red line represents the human trajectory and the green on shows the companion robot's trajectory. For most of the time, the robot follows the human from behind

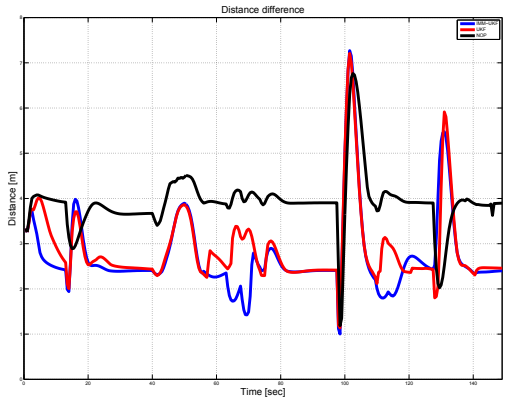

Fig. 7: Comparison of distance between the human and the robot using the MPC and the reactive methods

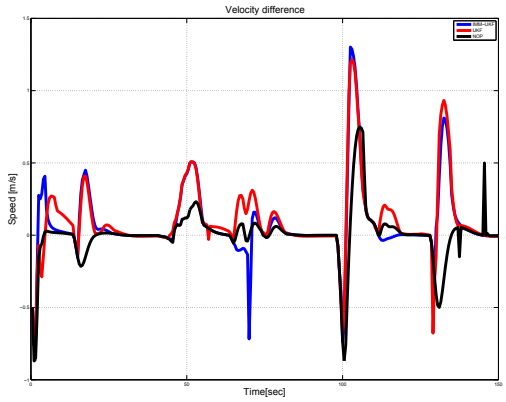

Fig. 8: Comparison of velocity difference between the human and the robot using the MPC and the reactive methods

but still within the comfort range using the former predictor than with the latter one. (**TODO:** if possible, still compare the portion that IMM-UKF and UKF make the robot stay in the comfort distance.)

The non-prediction method achieves smaller velocity difference than methods using predictors. This seems to imply that the non-prediction method is preferable for the robot to keep similar pace as the human. However, such similarity using non-prediction method results in large distance between the human and the robot, which is undesirable. The fluctuation in the velocity when using predictors is causes by the motion planner's effort to keep the robot within the comfort region around the human. Therefore, the simulation results show the superiority of using the multiple-model predictor (IMM-UKF predictor) for robot motion planning.

V. CONCLUSION

We have developed an autonomous motion planning approach for human-companion robots to accompany a target person in a socially desirable manner. Such companion robot can be useful for search and rescue scenarios by assisting humans in carrying apparatus, exploring dangerous areas and detecting survivors. The IMM-UKF approach that incorporates the uniform motion model and the coordinated turn motion models is proposed for human position estimation and prediction. Such multiple-model approach captures different human motion patterns, thus improving the estimation and prediction accuracy than other commonly-used single-model approaches. Based on the predicted human positions, the model predictive control (MPC) approach is utilized for planning robot motion trajectory, which considers the safety and comfort of the behavior. The estimation and prediction performance using IMM-UKF is compared with IMM-LKF and two single-model methods (LFK and UKF). Simulation results show superior accuracy and response speed in estimation and prediction using the IMM-UKF approach, especially when the human makes circular motion or sharp turns. Moreover, the MPC planner is evaluated using the IMM-UKF predictor, the UKF predictor and without predictor. The planner successfully ensures the safety of the accompanied person using all these prediction strategies. The IMM-UKF predictor improves the robot motion behavior by keeping the robot within the comfort distance range from the human.

In the future work, we plan to investigate other motion prediction methods, such as the auto-regressive moving-average (ARMA) method, and compare with IMM-UKF method. Besides, enabling the robot to learn human motion model in real time is an attractive topic and may provide more accurate human motion prediction and results in better human-companion behavior.

VI. APPENDIX

A. IMM-LKF Predictor

Similar to IMM-UKF, IMM-LKF works with two dynamic models: one is the uniform motion model; the other is the coordinated turn motion model. If the turn rate is a known constant in the coordinated turn motion model in **??**,

the human estimation procedure can be modeled with the discrete time linear state space system as follows:

$$x^h(k+1) = Ax^h(k) + B_w w(k) \tag{11a}$$
$$y^h(k) = Cx^h(k) + v(k) \tag{11b}$$

where $x^h(k)$ and $y^h(k)$ represent the human motion state and the observation, respectively, at the time step k; $w(k)$ and $v(k)$ represent process noise and measurement noise, respectively. $x^h(k)$ consists of four elements: $p_1^h, v_1^h, p_2^h, v_2^h$, where p_1^h, p_2^h denote the longitudinal and lateral position of the human and v_1^h, v_2^h the corresponding velocity. We use two Linear Kalman Filters in the IMM for human tracking, each corresponding to a different dynamics model: the uniform motion model and the turn motion model. Two models differ in the A matrix and w in Eq. (11a) while sharing the same B_w. In particular, we define the matrices as follows:

$$A_U = \begin{bmatrix} 1 & T & 0 & 0 \\ 0 & 1 & 0 & 0 \\ 0 & 0 & 1 & T \\ 0 & 0 & 0 & 1 \end{bmatrix}, \tag{12a}$$

$$A_T = \begin{bmatrix} 1 & \frac{\sin(\omega T)}{\omega} & 0 & \frac{1-\cos(\omega T)}{\omega} \\ 0 & \cos(\omega T) & 0 & -\sin(\omega T) \\ 0 & \frac{1-\cos(\omega T)}{\omega} & 1 & \frac{\sin(\omega T)}{\omega} \\ 0 & \sin(\omega T) & 0 & \cos(\omega T) \end{bmatrix}, \tag{12b}$$

$$B_w = \begin{bmatrix} \frac{T^2}{2} & T & 0 & 0 \\ 0 & 0 & \frac{T^2}{2} & T \end{bmatrix}, \tag{12c}$$

$$w_U \sim \mathcal{N}(0, Q_U)\ w_T \sim \mathcal{N}(0, Q_T) \tag{12d}$$

where A_U and A_T stand for the A matrices of the uniform motion model and turn motion model, respectively; w_U and w_T denote the process noise of the uniform motion model and turn motion model, respectively; T represents the sampling time; ω represents the constant turn rate.

We assume that only the human position can be measured. Therefore, the parameters in observation model Eq. (11b) can be defined as:

$$C = \begin{bmatrix} 1 & 0 & 0 & 0 \\ 0 & 0 & 1 & 0 \end{bmatrix}, \tag{13a}$$
$$v \sim \mathcal{N}(0, V) \tag{13b}$$

Above linear state space models are used in LKF and IMM-LKF in this paper. Moreover, we set the turn rate ω to be 0.1 rad/s as a known constant, in the turn motion model in IMM-LKF.

B. Approximating Static Obstacles

Static rectangular obstacles are approximated and analytically represented as ellipses, as shown in **??**. Let l and m be the length and width of a rectangular obstacle centered at the origin. Let Section VI-B represent the ellipse that encloses the obstacle in the way that the four vertices of the rectangle lie on the boundary of the ellipse.

$$\frac{x^2}{a^2} + \frac{y^2}{b^2} = 1$$

In addition, assume that the rectangle and ellipse have the same aspect ratio, which means $\frac{l}{m} = \frac{a}{b}$, then $a = \frac{l}{\sqrt{2}}$ and $b = \frac{m}{\sqrt{2}}$.

REFERENCES

[1] T. Kruse, A. K. Pandey, R. Alami, and A. Kirsch, "Human-aware robot navigation: A survey," *Robotics and Autonomous Systems*, vol. 61, no. 12, pp. 1726–1743, 2013.

[2] F. Hoeller, D. Schulz, M. Moors, and F. E. Schneider, "Accompanying persons with a mobile robot using motion prediction and probabilistic roadmaps," in *Intelligent Robots and Systems, 2007. IROS 2007. IEEE/RSJ International Conference on*, pp. 1260–1265, IEEE, 2007.

[3] D. Fox, W. Burgard, S. Thrun, *et al.*, "The dynamic window approach to collision avoidance," *IEEE Robotics & Automation Magazine*, vol. 4, no. 1, pp. 23–33, 1997.

[4] M. Svenstrup, T. Bak, and H. J. Andersen, "Trajectory planning for robots in dynamic human environments," in *Intelligent Robots and Systems (IROS), 2010 IEEE/RSJ International Conference on*, pp. 4293–4298, IEEE, 2010.

[5] E. T. Hall, R. L. Birdwhistell, B. Bock, P. Bohannan, A. R. Diebold Jr, M. Durbin, M. S. Edmonson, J. Fischer, D. Hymes, S. T. Kimball, *et al.*, "Proxemics [and comments and replies]," *Current anthropology*, pp. 83–108, 1968.

[6] M.-L. Barnaud, N. Morgado, R. Palluel-Germain, J. Diard, and A. Spalanzani, "Proxemics models for human-aware navigation in robotics: Grounding interaction and personal space models in experimental data from psychology," in *Proceedings of the 3rd IROS2014 workshop Assistance and Service Robotics in a Human Environment*, 2014.

[7] D. Koller, J. Weber, and J. Malik, *Robust multiple car tracking with occlusion reasoning*. Springer, 1994.

[8] A. Cosgun, D. Florencio, H. I. Christensen, *et al.*, "Autonomous person following for telepresence robots," in *Robotics and Automation (ICRA), 2013 IEEE International Conference on*, pp. 4335–4342, IEEE, 2013.

[9] A. Bruce and G. Gordon, "Better motion prediction for people-tracking," in *Proc. of the Int. Conf. on Robotics & Automation (ICRA), Barcelona, Spain*, 2004.

[10] M. Bennewitz, W. Burgard, G. Cielniak, and S. Thrun, "Learning motion patterns of people for compliant robot motion," *The International Journal of Robotics Research*, vol. 24, no. 1, pp. 31–48, 2005.

[11] C. Fulgenzi, C. Tay, A. Spalanzani, and C. Laugier, "Probabilistic navigation in dynamic environment using rapidly-exploring random trees and gaussian processes," in *Intelligent Robots and Systems, 2008. IROS 2008. IEEE/RSJ International Conference on*, pp. 1056–1062, IEEE, 2008.

[12] A. F. Foka and P. E. Trahanias, "Probabilistic autonomous robot navigation in dynamic environments with human motion prediction," *International Journal of Social Robotics*, vol. 2, no. 1, pp. 79–94, 2010.

[13] J. K. Aggarwal and Q. Cai, "Human motion analysis: A review," *Computer vision and image understanding*, vol. 73, no. 3, pp. 428–440, 1999.

[14] J. Rios-Martinez, A. Spalanzani, and C. Laugier, "Understanding human interaction for probabilistic autonomous navigation using risk-rrt approach," in *Intelligent Robots and Systems (IROS), 2011 IEEE/RSJ International Conference on*, pp. 2014–2019, IEEE, 2011.